RSC Advances

PAPER

View Article Online
View Journal | View Issue

Cite this: *RSC Adv.*, 2021, **11**, 36958

Magnetic sulfonated polysaccharides as efficient catalysts for synthesis of isoxazole-5-one derivatives possessing a substituted pyrrole ring, as anti-cancer agents†

Zarrin Ghasemi, *[a] Afsaneh Hamidian Amale,[a] Sajjad Azizi,[ab] Sepideh Valizadeh[a] and Jafar Soleymani[b]

Received 27th August 2021
Accepted 4th November 2021

DOI: 10.1039/d1ra06472j

rsc.li/rsc-advances

Four polysaccharides (chitosan, cellulose, starch, and pectin) were magnetized with magnetic iron oxide (Fe_3O_4) and then sulfonated (except pectin) with chlorosulfonic acid. The obtained solid acids were used as a catalyst in three-component reactions between *N*-substituted-2-formylpyrrole, hydroxylamine-hydrochloride, and β-keto esters for the synthesis of 4-(2-pyrrolyl) methylene-isoxazole-5-ones. The optimal catalyst system was selected and studied by IR, SEM, TEM and XRD methods. The diverse isoxazoline derivatives (obtained *via* a mild and simple approach) were also fully characterized by spectroscopic methods and screened for anti-cancer activities against HT-29 and MCF-7 colon and breast cancer and HEK 293 normal cells. The results revealed interesting anti-cancer activities.

Introduction

Structurally modified carbohydrates are of great interest due to their wide applications in physiological, industrial, and catalytic processes.[1,2] Meanwhile, functionally improved polysaccharides such as sulfonated backbones play important roles as heterogeneous catalysts in a variety of organic syntheses.[3–5] These $-SO_3H$ appended biopolymers with high acid site density as well as recyclability and biodegradability, could be efficient solid acid catalysts in many attractive multicomponent reactions.[6–8] Considering that magnetized substrates facilitate the separation process and reusability of the catalytic systems, their use has received special attention in improving the catalyst

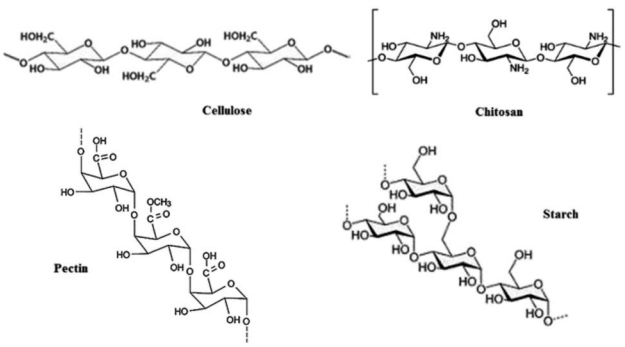

Fig. 2 Structures of studied polysaccharides in this work.

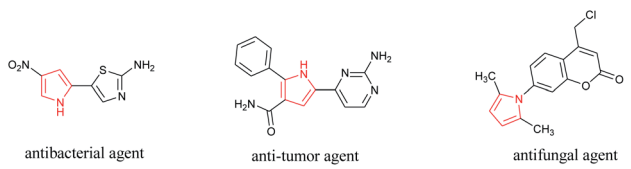

Fig. 1 Structure of pyrrole based bioactive compounds.

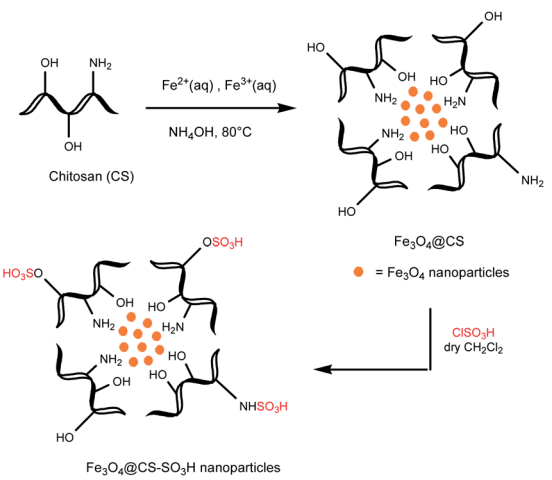

Scheme 1 Synthesis of Fe_3O_4@CS–SO_3H nanoparticles.

[a]*Department of Organic Chemistry and Biochemistry, Faculty of Chemistry, University of Tabriz, Tabriz 5166614766, Iran. E-mail: z.ghasemi@tabrizu.ac.ir*

[b]*Pharmaceutical Analysis Research Center, Tabriz University of Medical Sciences, Tabriz, Iran*

† Electronic supplementary information (ESI) available. See DOI: 10.1039/d1ra06472j

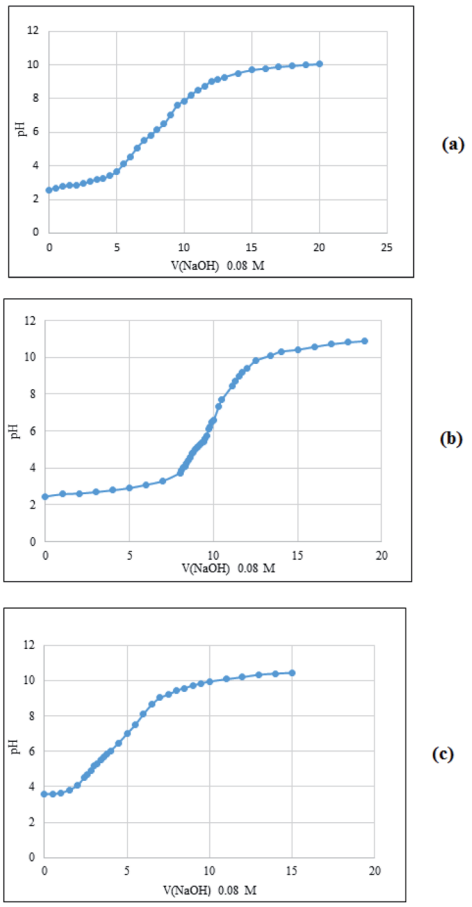

Fig. 3 The potentiometric curves of Fe_3O_4@chitosan–SO_3H (a), Fe_3O_4@cellulose–SO_3H (b), Fe_3O_4@starch–SO_3H (c).

structure.[9] Among the known multicomponent reactions, those leading to heterocyclic ring formation are particularly interesting. Isoxazole is a heterocycle ring with nitrogen and oxygen heteroatoms at the adjacent position whose derivatives are of great biological and medicinal importance[10–13] as well as optical and photochromic applications.[14,15] Isoxazol-5-ones are also one of the valuable synthetic targets because of their broad spectrum of pharmaceutical properties such as tyrosine inhibitory[16] and antitumor activity.[17,18] A catalytic one-pot reaction of aldehydes, β-ketoesters, and hydroxylamine-hydrochloride is the known method for the synthesis of these compounds.[19,20] The development of several synthetic methodologies by utilizing diverse catalytic substrates exhibits the growing interests into the synthesis of many isoxazole-5-one derivatives.[21–24] Various magnetic functionalized polysaccharides have been recently prepared by our group whose copper complexes showed high catalytic activities for the synthesis of diverse *N*-sulfonylamidine derivatives.[25–28] In this work we report the preparation and fully characterization of Fe_3O_4 magnetized sulfonated polysaccharides such as chitosan, cellulose and starch and evaluation of their catalytic activities in three-component reactions between *N*-substituted-pyrrole-2-carboxaldehyde, hydroxylamine-hydrochloride, and β-ketoesters to afford pyrrole containing isoxazole-5-ones. Since the hybrid molecules containing a pyrrole ring with other heterocyclic moiety, have shown biological activities such as antibacterial, anti-tumor, and antifungal (Fig. 1),[29–31] we used *N*-substituted-2-formylpyrrole as aldehyde partner at the mentioned reactions. The synthesized compounds were screened for anti-cancer activity against HT-29 and MCF-7 of colon and breast cancer and HEK 293 normal cells which the results are presented.

Results and discussion

Synthesis and characterization of magnetic sulfonated polysaccharides

In this work, we first prepared the magnetic polysaccharides based on chitosan, cellulose, starch and pectin.

Commercially available polysaccharide (Fig. 2) was treated with $FeCl_3 \cdot 6H_2O$ and $FeCl_2 \cdot 4H_2O$ (in a molar ratio 2 : 1) in the aqueous alkaline mixture at 80 °C to prepare magnetic solid, which was separated using an external magnetic field.[25,32–34] Magnetic product (Fe_3O_4@polymer) was then reacted with chlorosulfonic acid to form the sulfonated magnetic polymer (Fe_3O_4@polymer–SO_3H).[6,35,36] The typical route to prepare the chitosan based product is illustrated in Scheme 1. Pectin was not sulfonated in order to evaluate its ability to release of H^+ from the carboxylic acid groups and its catalytic proficiency without sulfonic acid groups.

We then used potentiometric titration to determine the acidity of the obtained solid acids. A mixture of solid acid (100 mg) in distilled water (25 mL) was stirred at room temperature for 24 hours and then dispersed with ultrasonic probe for 1 hour (frequency of 70 Hz). The mixture was then titrated with NaOH solution (0.08 N) and potentiometric curve was obtained (Fig. 3). According to data of the equivalence point, the acidity was calculated as shown in Table 1. As seen, the chitosan and cellulose based acids have a similar state in terms of initial pH and H^+ release power. The starch containing composite showed

Table 1 Potentiometric data of the functionalized polysaccharides

Solid acids	Primary pH	Volume of used NaOH solution up to the equivalence point (mL)	pH at the equivalence point	Acidity (mmol of H^+ per 100 mg solid acid)
Fe_3O_4@chitosan–SO_3H	2.58	8.5	6.49	0.7
Fe_3O_4@cellulose–SO_3H	2.45	9.9	6.47	0.8
Fe_3O_4@starch–SO_3H	3.57	4	6.03	0.3
Fe_3O_4@pectin	7.54	—	—	—

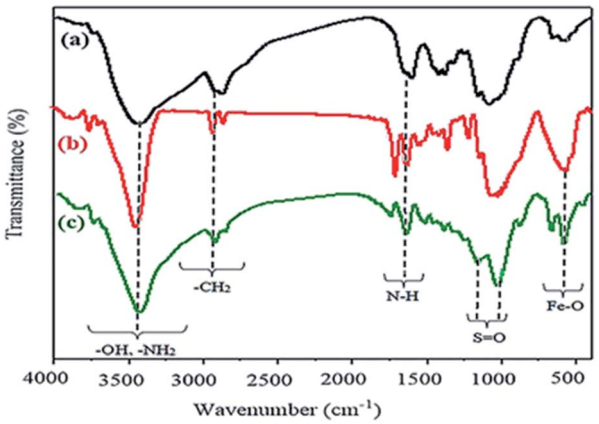

Fig. 4 FT-IR spectra for chitosan (a), Fe_3O_4@CS (b), and Fe_3O_4@CS–SO_3H (c).

the lower acidity and the pectin based acid was not be titrated due to its higher primary pH.

These solid acids were then used as heterogeneous catalysts in multi-component synthesis of pyrrole containing isoxazole-5-one derivatives. As will be seen, the catalyst containing chitosan showed higher catalytic activity than the others. For this reason, we report herein full characterization of this catalyst (Fe_3O_4@-chitosan–SO_3H) by IR, SEM, EDX, VSM, TEM, and XRD methods. Some information about the other three catalysts is given in the ESI.† Fig. 4 illustrates the FT-IR spectra of the generated species within the synthesis of the nanocatalyst. As shown in the FT-IR spectrum of chitosan (a), the strong and broad absorption band at around 3430 cm^{-1}, overlapped with the N–H stretching band, is related to the OH group. The bands at 2873 cm^{-1} and 1384 cm^{-1} are imputed to the C–H stretching vibrations of the CH_2 groups and the C–H bending vibrations, respectively. The particular signals for the amine (N–H) bending

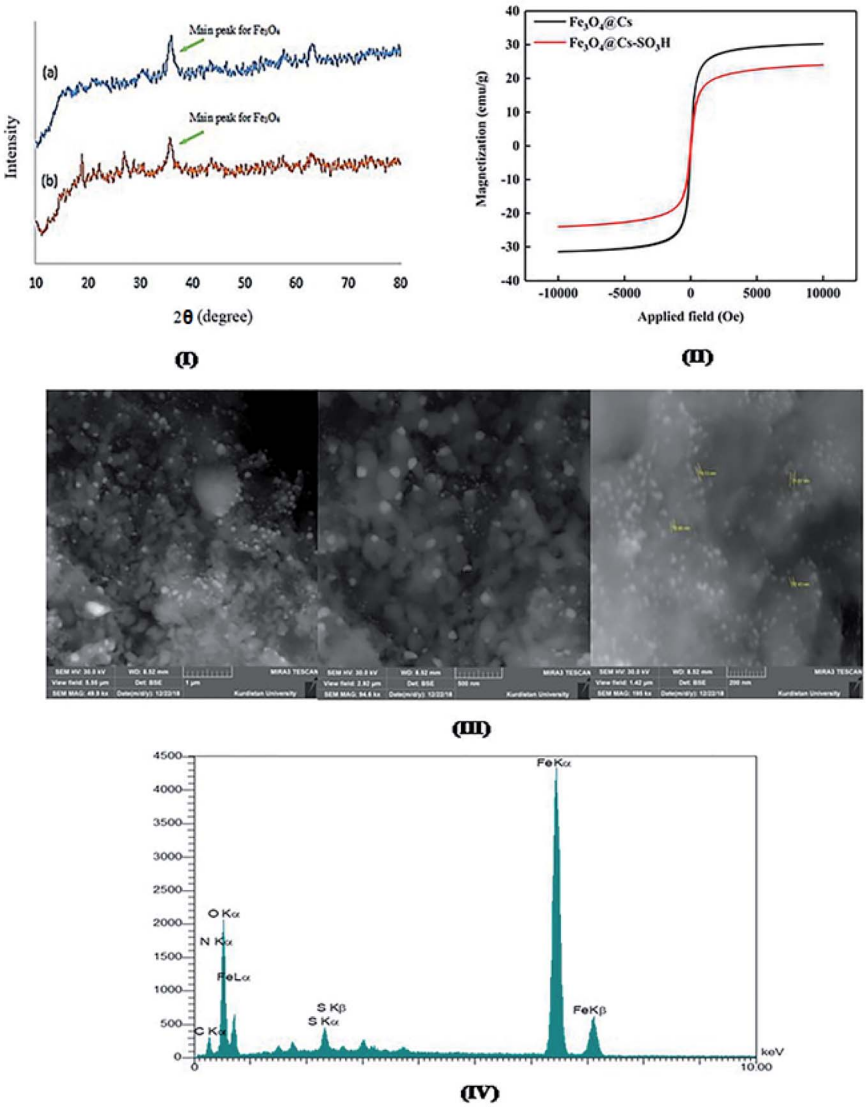

Fig. 5 (I) XRD patterns of Fe_3O_4@CS (a) and Fe_3O_4@CS–SO_3H (b); (II) magnetic hysteresis curves for prepared nanocomposites; (III) SEM images of the Fe_3O_4@chitosan–SO_3H: 1 μm (left), 500 nm (middle), 200 nm (right); (IV) EDX pattern of the Fe_3O_4@CS–SO_3H.

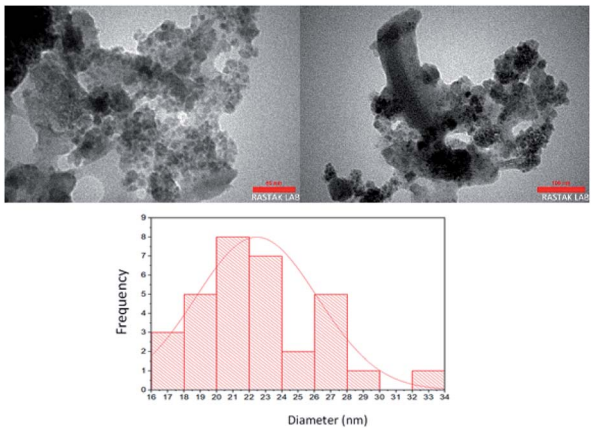

Fig. 6 TEM images of Fe_3O_4@chitosan–SO_3H.

vibration arise at 1606 cm^{-1} for chitosan. In the FT-IR spectrum of magnetic chitosan (b), absorption at 578 cm^{-1} assigned to the vibration of Fe–O in Fe_3O_4. The spectrum (c) also appears the absorption bands at 1249 and 1027 cm^{-1} which are ascribed to –S=O stretching vibration of –SO_3H groups.

The XRD patterns of the synthesized nanocatalysts were indicated in Fig. 5(I). The specific peaks of the catalyst at 2θ = 32.81, 35.68, 43.65, 53.38, 57.37, and 63.55 degrees are related to inverse cubic spinel magnetite (Fe_3O_4) crystal structure. No improbity in the XRD patterns suggests the foundation of pure Fe_3O_4 nanoparticles. The weak and small broad bands (curve b) in the range of 2θ = 25–28 represent the entity of amorphous sulfonated chitosan. The quantity of magnetization saturation of the Fe_3O_4@CS and Fe_3O_4@CS–SO_3H nanocomposites was obtained using a vibrating sample magnetometer at room temperature with values 30.25 and 20.03 emu g^{-1} respectively (Fig. 5(II)). These results demonstrate that the catalyst is paramagnetic and consequently can be easily separated from the reaction medium through an external magnetic field and reused. Fig. 5(III) also shows the surface morphology and particle size distribution of the catalyst that were studied by SEM analysis. The SEM images illustrate the uniform dispersity of spherical particles and also the attendance of Fe_3O_4 on chitosan support with average particle size of 9–15 nm. The EDX spectroscopy was carried out to study the incidence of elemental signals of prepared Fe_3O_4@CS–SO_3H nanocomposite (Fig. 5(IV)). The results illustrate the presence of N, O, C, Fe, and S elements in the nanocatalyst and confirm that chitosan polymer is covered on the surface of iron oxide nanoparticles.

The TEM micrograph of the Fe_3O_4@chitosan–SO_3H which is shown in Fig. 6, reveals the distribution of Fe_3O_4 particles on functionalized chitosan. The size of nanoparticles was calculated using image J software to be approximately 22 nm.

Application of the catalysts towards one-pot synthesis of the novel isoxazole-5-one derivatives

We used commercial pyrrole-2-carbaldehyde **1a** and its *N*-methyl derivative **1b** as well as the prepared *N*-substituted derivatives **1c–e** (Scheme 2), as aldehyde partner in the desired

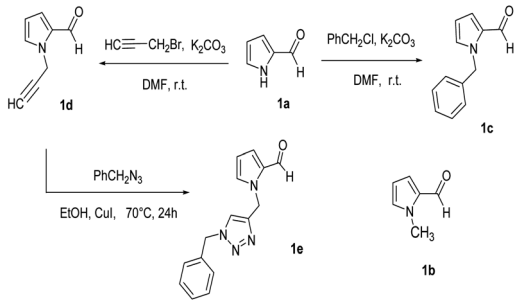

Scheme 2 The preparation of aldehyde precursors.

three-component reactions. As shown, substitution reactions of **1a** with benzyl chloride or propargyl bromide in the presence of K_2CO_3 in DMF gave the compounds **1c** [37] and **1d** [38] respectively. CuI catalyzed 1,3-dipolar cycloaddition of **1d** with benzyl azide,[39] resulted in the new triazole derivative **1e**. Three-component reaction between 1-benzylpyrrole-2-carboxaldehyde **1c**, hydroxylamine-hydrochloride and methyl acetoacetate to obtain product **3e**, was selected as a model to optimize reaction conditions (Table 2). Initially, four kinds of magnetic catalysts containing Fe_3O_4@chitosan–SO_3H, Fe_3O_4@cellulose–SO_3H, Fe_3O_4@starch–SO_3H, and Fe_3O_4@pectin were examined in equal amounts (0.04 g) per 1 mmol of aldehyde component (entries 1–4). As shown, the chitosan containing catalyst resulted in higher yield of **3e** (89%) at shorter time (2 hours). Changing the amount of this catalyst did not improve the result (entries 5 and 6). Although solvent-free conditions reduced the yield of the product (entry 8), the use of ethanol had a good effect (entry 7) and even was better when using ethyl benzoyl acetate as β-ketoester. The use of other solvent such as THF and CH_2Cl_2 increased the purification

Table 2 Optimization of the reaction conditions[a]

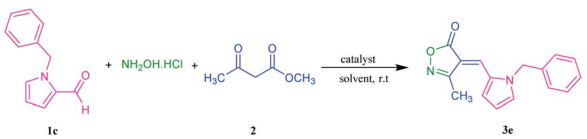

Entry	Catalyst (mg)	Solvent	Time (h)	Yield[b] (%)
1	Fe_3O_4@pectin (40)	H_2O	5	58
2	Fe_3O_4@starch–SO_3H (40)	H_2O	3	65
3	Fe_3O_4@cellulose–SO_3H (40)	H_2O	2	82
4	Fe_3O_4@chitosan–SO_3H (40)	H_2O	2	89
5	Fe_3O_4@chitosan–SO_3H (50)	H_2O	2	89
6	Fe_3O_4@chitosan–SO_3H (30)	H_2O	3	75
7	Fe_3O_4@chitosan–SO_3H (40)	EtOH	2	88
8	Fe_3O_4@chitosan–SO_3H (40)	Solvent-free	2	30
9	Fe_3O_4@chitosan–SO_3H (40)	THF	2	63
10	Fe_3O_4@chitosan–SO_3H (40)	CH_2Cl_2	2	59

[a] Reaction conditions: aldehyde (1 mmol), hydroxylamine hydrochloride (1.5 mmol), β-keto ester (1.5 mmol), room temperature, solvent (10 mL). [b] Isolated yields.

steps and reduced the yield of **3e** (entries 9 and 10). Three-component condensation of *N*-substituted-2-formylpyrrole **1a–e**, hydroxylamine hydrochloride, and β-keto ester **2a,b** in the presence of Fe_3O_4@chitosan–SO_3H in EtOH or H_2O at room temperature, gave a series of 4-(2-pyrrolyl)methylene-isoxazole-5-ones **3a–j** in good to excellent yields (Table 3). 5-Methylfuran-2-carboxaldehyde was also applied as aldehyde partner in this reaction and product **3k** was obtained as yellow solid.

It is undeniable that the recovery and reuse of catalysts are important for a catalytic procedure. In this regard, the recyclability of the Fe_3O_4@chitosan–SO_3H was explored using the model reaction of *N*-benzyl-2-formylpyrrole **1c**, hydroxylamine hydrochloride, and methyl acetoacetate under identical reaction conditions. Once the reaction is complete, the recovered magnetic nanocatalyst was washed with ethanol, dried at room

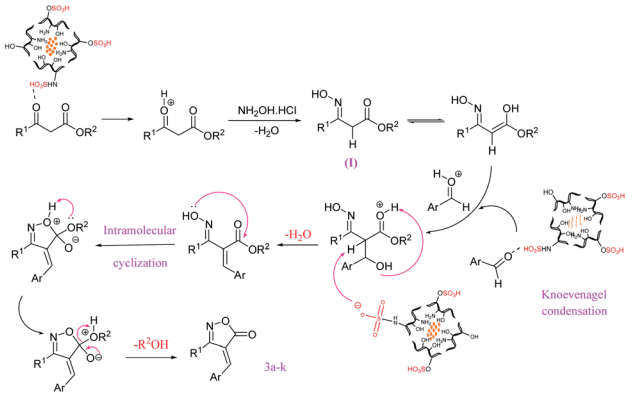

Fig. 7 The proposed mechanism for the formation of isoxazole-5-(4*H*)-one derivatives.

Table 3 Synthesis of isoxazole-5-(4*H*)-one derivatives **3a–k** in the presence of Fe_3O_4@chitosan–SO_3H[a,b]

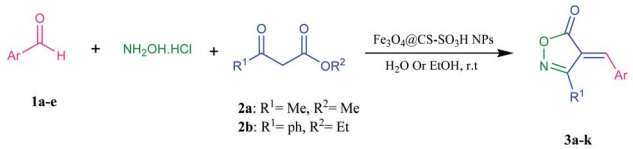

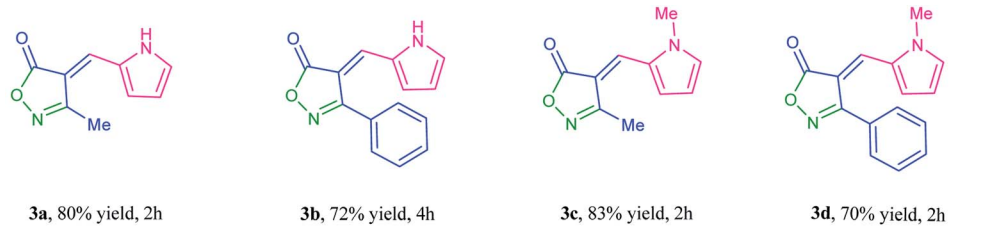

3a, 80% yield, 2h **3b**, 72% yield, 4h **3c**, 83% yield, 2h **3d**, 70% yield, 2h

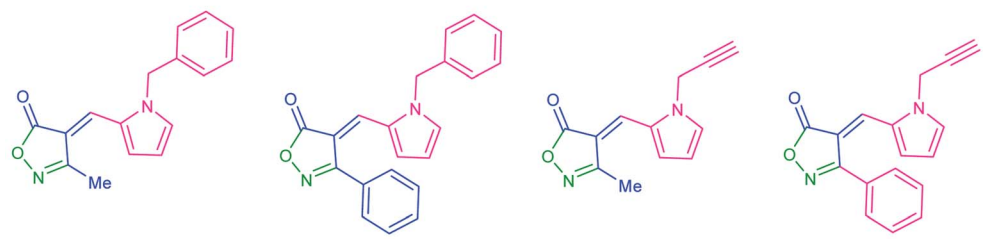

3e, 89% yield, 2h **3f**, 80% yield, 2h **3g**, 85% yield, 2h **3h**, 80% yield, 3h

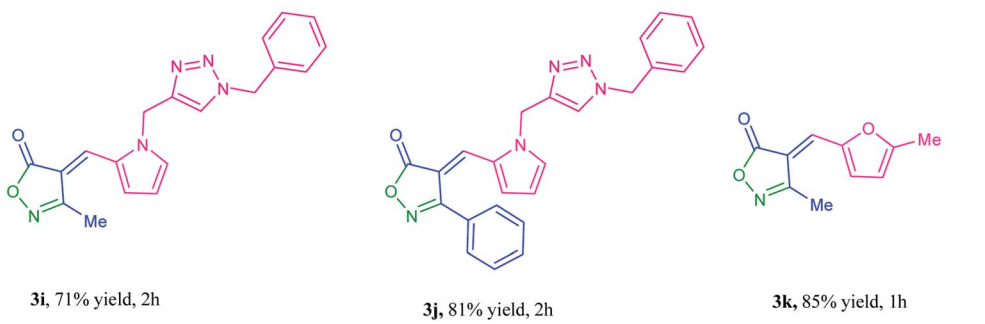

3i, 71% yield, 2h **3j**, 81% yield, 2h **3k**, 85% yield, 1h

[a] Isolated yield. [b] The reactions were carried out with **1a–c** (1 mmol), β-keto ester **2** (1.5 mmol), hydroxylamine hydrochloride (1.5 mmol) in ethanol or water (10 mL) at room temperature.

temperature, and reused for more runs. Heterogeneous and magnetic property of the Fe_3O_4@chitosan–SO_3H which facilitates the recovery of the nanocatalyst from the reaction mixture by an external magnet, allowed recyclization and four times reuse the catalyst. The obtained yields in these 4 uses were: 89%, 85%, 81% and 78% for product **3e**. A possible mechanism for the synthesis of isoxazole-5-(4*H*)-one, in the presence of Fe_3O_4@CS–SO_3H, is shown in Fig. 7. In the first step, acid catalyst protonates the carbonyl group of β-ketoester and activates it for condensation with hydroxylamine to give oxime (**I**). In the next step, activated aromatic aldehyde reacts with the oxime intermediate through Knoevenagel condensation. Finally, the desired product **3a–k** was obtained by intramolecular cyclization and elimination of alcohol.

Biological studies

The synthesized 4-arylmethylene-isoxazol-5(4*H*)-ones **3a–k** were examined for cell cytotoxicity analyses against three different cancer cell lines: normal cell (HEK 293), human colon adenocarcinoma (HT-29) and human breast adenocarcinoma (MCF-7) using the MTT assay.[40–44] Afterward, doxorubicin was utilized as a prominent anticancer medicine for positive control of this research. The antiproliferative efficacy values are used as IC_{50} which are regarded as the levels of the synthesized materials that cause about 50% cell proliferation (Table 4). The IC_{50} values of at least three separated experiments were averaged. Cell viability was measured through MTT assay as described in the methods subsection. The examination of cytotoxicity properties of the compounds **3a–k** showed that all of eleven desired compounds possessed cytotoxicity activity against MCF-7 and HT-29 cancer cell lines. The compounds **3b**, **3e**, **3f**, **3h**, **3j** and **3k** exhibited good cytotoxicity activities against MCF-7 cell line and the compounds **3b**, **3f**, **3h** and **3k** against HT-29 cell line. It has been obvious that the derivative **3k** containing furan ring indicated remarkable cytotoxic activity against both HT-29 and MCF-7 cell lines (Table 4). Moreover, the cytotoxicity activities of desired compounds **3a–k** against HEK 293 normal cells were also investigated and the results showed poor cytotoxic effects. The cytotoxic activities of all derivatives have been graphically exhibited in Fig. 8.

Table 4 IC_{50} (μM) of the synthesized compounds against different cancer cell lines

Product	MCF-7	HT-29	HEK 293
3a	10	12	102
3b	3	10	98
3c	7	15	189
3d	5	13	201
3e	4	15	167
3f	3	10	79
3g	5	15	94
3h	4	10	109
3i	7	18	171
3j	4	15	128
3k	2	10	101
Doxorubicin	2.4 ± 0.12	0.49	1.30

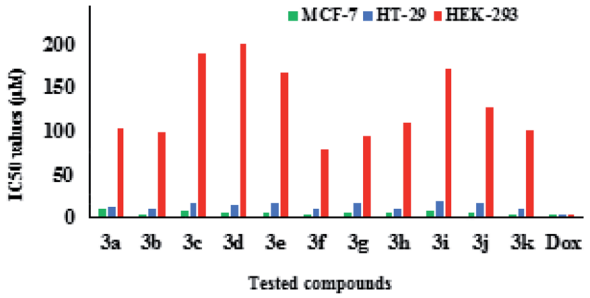

Fig. 8 Graphical presentation of the cytotoxic activity of the 4-arylmethylene-isoxazole-5(4*H*)-ones.

Conclusions

We report in this research, the use of Fe_3O_4 incorporated sulfonated polysaccharides as solid acid catalysts for the synthesis of novel isoxazole-5-one derivatives comprising substituted pyrrole ring. The three-component reactions of *N*-substituted-2-formylpyrrole, hydroxylamine-hydrochloride, and β-ketoesters under optimized conditions (in the presence of chitosan based catalyst) resulted in the desired products in good yields. The obtained products **3a–k** were also examined for cell cytotoxicity analyses against human colon adenocarcinoma (HT-29) and human breast adenocarcinoma (MCF-7) using the MTT assay. The results showed good cytotoxicity for compounds **3b**, **3f**, **3h** and **3k** and relatively poor cytotoxicity against HEK 293 normal cells.

Conflicts of interest

There are no conflicts to declare.

Acknowledgements

This project has been supported by a research grant from the University of Tabriz (number: 793). The authors are grateful for the research interests of the University of Tabriz for this grant.

Notes and references

1 H. E. Caputo, J. E. Straub and M. W. Grinstaff, *Chem. Soc. Rev.*, 2019, **48**, 2338–2365.
2 R. Mahajan, R. Mahajan, A. Selim, K. M. Neethu, S. Sharma, V. Shanmugam and G. Jayamurugan, *Nanotechnol.*, 2021, **32**, 475704–475716.
3 A. Pourjavadi, F. Seidi, S. S. Afjeh, N. Nikoseresht, H. Salimi and N. Nemati, *Starch/Staerke*, 2011, **63**, 780–791.
4 A. Shaabani, A. Rahmati and Z. Badri, *Catal. Commun.*, 2008, **9**, 13–16.
5 I. M. Lokman, U. Rashid and Y. H. Taufiq-Yap, *Arabian J. Chem.*, 2016, **9**, 179–189.
6 A. Maleki, E. Akhlaghi and R. Paydar, *Appl. Organomet. Chem.*, 2016, **30**, 382–386.
7 M. Mamaghani, K. Tabatabaeian, M. Mohammadi and A. Khorshidi, *J. Chem.*, 2013, **2013**, 1–6.

8 A. Shaabani, A. Maleki, J. M. Rad and E. Soleimani, *Chem. Pharm. Bull.*, 2007, **55**, 957–958.
9 K. Hasan, I. A. Shehadi, N. D. Al-Bab and A. Elgamouz, *Catal*, 2019, **9**, 839–856.
10 C. Altug, H. Güneş, A. Nocentini, S. M. Monti, M. Buonanno and C. T. Supuran, *Bioorg. Med. Chem.*, 2017, **25**, 1456–1464.
11 C. Changtam, P. Hongmanee and A. Suksamrarn, *Eur. J. Med. Chem.*, 2010, **45**, 4446–4457.
12 P. Diana, A. Carbone, P. Barraja, G. Kelter, H.-H. Fiebig and G. Cirrincione, *Bioorg. Med. Chem.*, 2010, **18**, 4524–4529.
13 S. Suryawanshi, A. Tiwari, N. Chandra and S. Gupta, *Bioorg. Med. Chem. Lett.*, 2012, **22**, 6559–6562.
14 G. Liu, M. Liu, S. Pu, C. Fan and S. Cui, *Tetrahedron*, 2012, **68**, 2267–2275.
15 X.-H. Zhang, Y.-H. Zhan, D. Chen, F. Wang and L.-Y. Wang, *Dyes Pigm.*, 2012, **93**, 1408–1415.
16 S. J. Kim, J. Yang, S. Lee, C. Park, D. Kang, J. Akter, S. Ullah, Y.-J. Kim, P. Chun and H. R. Moon, *Bioorg. Med. Chem.*, 2018, **26**, 3882–3889.
17 S. K. Laughlin, M. P. Clark, J. F. Djung, A. Golebiowski, T. A. Brugel, M. Sabat, R. G. Bookland, M. J. Laufersweiler, J. C. VanRens and J. A. Townes, *Bioorg. Med. Chem. Lett.*, 2005, **15**, 2399–2403.
18 S. Rollas, Ş. Kokyan, B. K. Kaymakçıoğlu, S. Ö. Turan and J. Akbuğa, *Marmara Pharm. J.*, 2011, **15**, 94–99.
19 F. Saikh, J. Das and S. Ghosh, *Tetrahedron Lett.*, 2013, **54**, 4679–4682.
20 M. Parveen, A. Aslam, A. Ahmad, M. Alam, M. R. Silva and P. P. Silva, *J. Mol. Struct.*, 2020, **1200**, 127067.
21 M. Ahmadzadeh, Z. Zarnegar and J. Safari, *Green Chem. Lett. Rev.*, 2018, **11**, 78–85.
22 H. Kiyani and F. Ghorbani, *J. Saudi Chem. Soc.*, 2017, **21**, S112–S119.
23 S. Fozooni, N. G. Hosseinzadeh, H. Hamidian and M. R. Akhgar, *J. Braz. Chem. Soc.*, 2013, **24**, 1649–1655.
24 Q. Liu and R.-T. Wu, *J. Chem. Res.*, 2011, **35**, 598–599.
25 Z. Ghasemi, S. Shojaei and A. Shahrisa, *RSC Adv.*, 2016, **6**, 56213–56224.
26 S. Shojaei, Z. Ghasemi and A. Shahrisa, *Appl. Organomet. Chem.*, 2017, **31**, 3788–3807.
27 S. Shojaei, Z. Ghasemi and A. Shahrisa, *Tetrahedron Lett.*, 2017, **58**, 3957–3965.
28 S. Valizadeh, Z. Ghasemi, A. Shahrisa, B. Notash, M. Pirouzmand and R. Kabiri, *Carbohydr. Polym.*, 2019, **226**, 115310–115320.
29 S.-G. Zhang, C.-G. Liang, Y.-Q. Sun, P. Teng, J.-Q. Wang and W.-H. Zhang, *Mol. Diversity*, 2019, **23**, 915–925.
30 V. Bhardwaj, D. Gumber, V. Abbot, S. Dhiman and P. Sharma, *RSC Adv.*, 2015, **5**, 15233–15266.
31 R. A. Rane, P. Bangalore, S. D. Borhade and P. K. Khandare, *Eur. J. Med. Chem.*, 2013, **70**, 49–58.
32 H. Naeimi and S. Lahouti, *J. Iran. Chem. Soc.*, 2018, **15**, 2017–2031.
33 C. P. Okoli, E. B. Naidoo and A. E. Ofomaja, *Environ. Nanotechnol. Monit. Manag.*, 2018, **9**, 141–153.
34 O. A. Attallah, M. A. Al-Ghobashy, M. Nebsen, R. El-Kholy and M. Y. Salem, *Environ. Sci. Pollut. Res.*, 2018, **25**, 18476–18483.
35 J. Safari, P. Aftabi, M. Ahmadzadeh, M. Sadeghi and Z. Zarnegar, *J. Mol. Struct.*, 2017, **1142**, 33–39.
36 R. Mohammadi and M. Z. Kassaee, *J. Mol. Catal. A: Chem.*, 2013, **380**, 152–158.
37 R. Di Santo, R. Costi, M. Artico, R. Ragno, G. Greco, E. Novellino, C. Marchand and Y. Pommier, *Il Farmaco*, 2005, **60**, 409–417.
38 P. R. Loaiza, S. Löber, H. Hübner and P. Gmeiner, *Bioorg. Med. Chem.*, 2007, **15**, 7248–7257.
39 For preparation of benzyl azide from reaction of benzyl chloride and sodium azide, see: T. Miao and L. Wang, *Synthesis*, 2008, **2008**, 363–368.
40 S. Azizi, J. Soleymani and M. Hasanzadeh, *Appl. Organomet. Chem.*, 2020, **34**, e5440.
41 Z. Ghasemi, S. Azizi, R. Salehi and H. S. Kafil, *Monatsh. Chem.*, 2018, **149**, 149–157.
42 S. Azizi, J. Soleymani and N. Shadjou, *J. Mol. Recognit.*, 2020, **33**, e2871.
43 M. Pirouzmand, P. S. Sani, Z. Ghasemi and S. Azizi, *J. Biol. Inorg Chem.*, 2020, **25**, 411–417.
44 E. F. Oskuie, S. Azizi, Z. Ghasemi, M. Pirouzmand, B. N. Kojanag and J. Soleymani, *Monatsh. Chem.*, 2020, **151**, 243–249.